Acta Manilana 72 (2024), 33-54

ISSN: 0065-1370

Acta Manilana

journal homepage: https://actamanilana.ust.edu.ph/

Predicted Inflammatory Protein Targets of *Tinospora cordifolia* Secondary Metabolites: ADMET and Molecular Docking Studies

Loraine Jewel P. Burayag[1], Yara Haifa R. Acmad[1], Carmela P. Alberto[1], Bernadette Nicole F. Ang[1], Marie Ericka V. Arona[1], Vincent Raphael R. Balajadia[1], Giselle Ann R. Bautista[1], Alanis Renei L. Berja[1], Jamille Anne C. Caringal[1], Alessandra E. Castillo[1], Maria Salvacion A. Esmalla[2], and Agnes L. Castillo[1,3,4]*

[1]Department of Pharmacy, Faculty of Pharmacy, University of Santo Tomas
[2]Department of Biochemistry, Faculty of Pharmacy, University of Santo Tomas
[3]Research Center for the Natural and Applied Sciences, University of Santo Tomas, España, Manila, Philippines
[4]The Graduate School, University of Santo Tomas, España, Manila, Philippines

Graphical Abstract

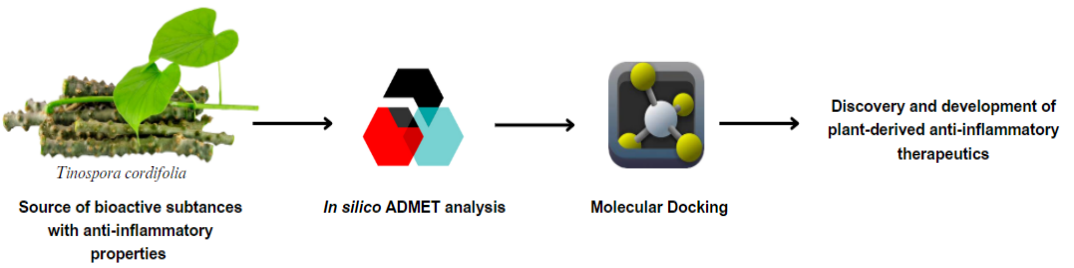

Abstract

Tinospora cordifolia received significant attention due to its medicinal and pharmacological properties in the treatment of various diseases. However, despite its well-established reputation for its anti-inflammatory effects, our understanding of the molecular mechanisms underlying these activities remains limited. To address this gap, an extensive literature review and identification of thirteen anti-inflammatory metabolites derived from *Tinospora cordifolia* was conducted. These metabolites were subjected to pharmacokinetic prediction using SwissADME and Protox II. Molecular docking techniques with DockingPie through PyMOL was also used to investigate their interactions with thirty-two proteins associated with different inflammatory pathways. Among the secondary metabolites tested, there were 14 conformations consisting of 13 proteins and 5 ligands which showed ideal binding affinity. Stigmasterol (11) had the greatest number of acceptable binding affinities among the 5 ligands with MMP-13 (-9.8 kcal/mol), Nf-kb1 (-8.6 kcal/mol), NIK (-8.2 kcal/mol), IL-17A (-8.2 kcal/mol), and TGF-B (-8.1 kcal/mol), followed by β-sitosterol (2) with COX-1 (-8.8 kcal/mol), LT-B (-8.8 kcal/mol), 15-LOX (-8.4 kcal/mol), and NIK (-8.2 kcal/mol).

Corresponding author: alcastillo@ust.edu.ph
DOI: https://doi.org/10.53603/actamanil.72.2024.esli3249

Date Received: 01 February 2024
Date Revised: 20 March 2024
Date Accepted: 21 March 2024

Then columbin (5) with 5-LOX (-8.5 kcal/mol), MMP-1 (-8.3 kcal/mol), and MMP-8 (-8.2 kcal/mol). Both berberine (3) and 20-hydroxyecdysone (1) are bound to the least number of proteins, namely MMP-2 (-8.9 kcal/mol) and MMP-19 (-8.9 kcal/mol), respectively. Meanwhile, ADMET analysis revealed that berberine (3), magnoflorine (7), menisperine (8), reticuline (10), and stigmasterol (11) are of good oral bioavailability, while β-sitosterol (2), syringin (12), and 20-hydroxyecdysone (1) have undesirable lipophilicity and polarity. Berberine (3), columbamine (4), jatrorrhizine (6), and palmatine (9) are predicted to be the most toxic compounds when administered via oral route. While these secondary metabolites exhibited optimal binding affinities, their potential as lead compounds is constrained by their drug-likeness properties, with some of them having violations in XLOGP3, MLOGP, and hydrogen bond following Lipinski's rule of five and Muegge's rule. Therefore, further functionalization and modification are imperative for prospective drug discovery and design.

Keywords: ADMET; Anti-inflammatory; Inflammation pathway; Molecular Docking; *Tinospora cordifolia*

Introduction

Inflammation is the body's natural response to foreign stimuli, injury, or infection as its defense mechanism. However, its uncontrolled persistence over time progresses into a chronic inflammation leading to serious health problems. Chronic inflammatory diseases such as stroke, respiratory diseases, cancer, and diabetes are considered one of the leading causes of death worldwide, with 3 out of 5 people dying [1]. Thus, the discovery and development of natural and synthetic drugs with anti-inflammatory activity remain crucial.

Natural products are recognized for their extensive pharmacological activities and minimal toxicity, which is beneficial for the development of natural anti-inflammatory drugs. Although most of the severe symptoms of chronic diseases cannot be treated with natural products, they can be used to alleviate pain during the early stage of the disease [2].

Tinospora cordifolia is a natural product used in various herbal preparations for treating different illnesses for its anti-periodic, antispasmodic, anti-microbial, anti- osteoporotic, anti-inflammatory, anti- arthritic, anti-allergic, and antidiabetic properties [3]. Several studies on the anti-inflammatory properties of *Tinospora cordifolia* have been reported, citing its remarkable activity in treating inflammatory disorders [4]. Sumanlata et al. (2019) also established that the aqueous extracts of *Tinospora cordifolia* exhibited highly effective and dose-related anti-inflammatory activities [5]. It was demonstrated that flavonoid contents of the plant and other mediators were able to inhibit prostaglandins, isoforms of inducible nitric oxide synthase (iNOS), and cyclooxygenase-2 (COX-2) enzymes induced from the inflammation. Moreover, Jacob and Kumar (2015) reported the dual inhibition of COX and lipoxygenase (LOX) enzymes in the presence of alkaloid and flavonoid phytoconstituents of *Tinospora cordifolia* [6]. Other important products of both pathways, including prostacyclins, thromboxanes, leukotrienes, and hydroperoxyeicosatetraenoic acid (HPETE), were found to be suppressed by the plant extracts.

Another study conducted by Philip, Tom, and Vasumathi (2018), wherein the chloroform extracts of *Tinospora cordifolia* (CETC) exhibited a significant suppression in cytokine secretion, transcription, and translation of proinflammatory biomarkers of macrophages exposed to lipopolysaccharide (LPS). This was further validated by CETC also producing a suppressive effect in the inflammatory late phase reactions in the rat model of carrageenan-induced hind paw edema, through inhibiting cyclooxygenase-2 [7]. Nevertheless, there remains a gap in our understanding of the molecular level anti-inflammatory mechanisms of *Tinospora cordifolia*, primarily because previous research works have focused solely on testing extracts of the plant rather than its individual components. Thus, this study is conducted to identify the specific secondary metabolites responsible for the anti-inflammatory activity of *Tinospora cordifolia*. Moreover, given the recognized inhibitory properties of the constituents in *Tinospora cordifolia*, there is a promising avenue to investigate its compounds as potential anti-inflammatory lead candidates. Through *in silico* investigations using molecular docking, and ADMET predictions, this research could lead to therapeutic advancement and personalized medicine that is beneficial to the scientific community and pharmaceutical industry.

Materials and methods

Protein Selection and Ligand Selection. Three inflammatory pathways were chosen for this study: the Arachidonic acid (AA) pathway, Nf-κb pathway, Matrix Metalloproteinases (MMP), and several Tumor Necrosis factors and interleukins. The selection of the AA pathway was based on its association with prevalent inflammatory conditions such as arthritis and asthma. This pathway is crucial in the inflammatory response as it facilitates the production of prostaglandins and leukotrienes. Consequently, a total of five target proteins were selected in the Arachidonic acid pathway which are the Cyclooxygenase-1 (COX-1), Cyclooxygenase-2 (COX-2), 5-Lipoxygenase (5-LOX), 12-Lipoxygenase (12-LOX) and 15-Lipoxygenase (15-LOX). On the other hand, the decision to focus on the NF-κB pathway and MMP was driven by their roles in regulating pro-inflammatory genes, including cytokines and chemokines, as well as in the activation and differentiation of immune cells. Specifically, three target proteins were selected for the Nf-κb pathway, namely, the Nf-κb1, RelA (p65), and NIK, while seven from the MMPs were chosen, which are MMP-1, MMP-2, MMP-8, MMP-9, MMP-13, MMP-19, and MMP-26. Finally, interleukins (ILs) were chosen for their pivotal role in activating immunological and inflammatory responses. Similarly, tumor necrosis factors were selected due to their crucial function in regulating the expression of inflammation, particularly by stimulating the production of macrophages. For the interleukins (ILs), the following were selected: IL-1α, IL-1β, IL-18, IL-2, IL- 4, IL-5, IL-6, IL-8, IL-13, IL-17A, and IL-17B, while there were five proteins selected from the Tumor Necrosis Factors, namely, TNF-α, TNF-β, CD40L, LT-β, and BAFF. The following target proteins have been selected meticulously considering their capacity to regulate the expression of inflammation and the abundance of studies supporting their inflammatory characteristics. All 3D structures of the proteins were obtained from RCSB Protein Data Bank (PDB) and UniProt.

For the ligands, the secondary metabolites from *Tinospora cordifolia* were screened based on extensive literature mapping to distinguish those compounds that exhibit anti-inflammatory properties. Hence, 20-Hydroxyecdysone (1), β-sitosterol (2), berberine (3), columbamine (4), columbin (5), jatrorrhizine (6), magnoflorine (7), menisperine (8), palmatine (9), reticuline (10), stigmasterol (11), syringin (12), and tetrahydropalmatine (THP) (13) were selected. Their structural models and canonical simplified molecular-input line-entry systems (SMILES) were obtained from the PubChem database.

SwissADME and ProTox II Analysis. SMILES format of each ligand was used in conducting SwissADME for the identification of its Absorption, Distribution, Metabolism, Excretion (ADME) profile; and Protox II for toxicity profile. Generated computational results were analyzed based on the scientific report by Daina, Michielin, and Zoete (2017) [8].

Molecular Docking. Protein structures collected from RCSB PDB and UniProt in PDB file format were optimized through PyMOL by removing bound ligands and water molecules [9] and adding missing polar hydrogens, if necessary [10]. Meanwhile, selected ligands collected from PubChem in SDF file format were subjected to Avogadro software for minimization of energy. Subsequently, the ligands were converted to PDB format.

After structure optimization, molecular docking has been performed using DockingPie through PyMOL. The grid parameters for each protein were modified to cover the whole molecule, and 20 poses were generated per each protein-ligand complex. The ligands with the best binding affinity from the set of docking poses were chosen to represent the set and subjected to post-docking analysis [10]. Results were placed in the visualizer panel of PyMOL and BIOVIA Discovery Studio, along with the target proteins.

Results and Discussion

SwissADME Prediction of Target Metabolites. Based on Table 1, berberine (3), magnoflorine (7), menisperine (8), reticuline (10), and stigmasterol (11) are within the accepted range of saturation, size, polarity, solubility, flexibility, and lipophilicity. All these molecules, therefore, indicate good oral bioavailability. However, the lipophilicity of β-sitosterol (2) has values beyond the specified range at 9.34. This is not desirable since it could result in poorer aqueous solubility in the gastrointestinal tract and reduced cell penetration [11]. Elevated levels of lipophilicity also indicate that these compounds have less oral bioavailability and are prone to enzymatic metabolism. Likewise, syringin (12) has a polarity value of 138.07 and 20-hydroxyecdysone (1) with 138.45, which are beyond the specified range. Highly polar substances may possibly lower lipophilicity, which may affect permeability [12]. Therefore, these predictions signify that syringin (12) and 20-hydroxyecdysone (1) are not orally bioavailable.

Table 1. SwissADME Prediction of Physicochemical Analysis of the Target Metabolites of *Tinospora cordifolia*

Compound	Saturation (≥ 0.25)	Size (g/mol) 150-500	Polarity (Å²) 20-130	Solubility (≤ 6)	Flexibility (< 9)	Lipophilicity (-0.7 - +6.0)
20-Hydroxyecdysone	0.89	480.63	**138.45**	-2.78	5	0.46
β-sitosterol	0.93	414.71	20.23	- 7.90	6	**9.34**
Berberine	0.25	336.36	40.80	-4.55	2	3.62
Columbamine	0.25	338.38	51.80	- 4.37	3	3.42
Columbin	0.60	358.39	85.97	- 3.50	1	2.16
Jatrorrhizine	0.25	338.38	51.80	-4.37	3	3.42
Magnoflorine	0.40	342.41	58.92	- 3.91	2	2.74
Menisperine	0.43	356.44	47.92	- 9.25	3	- 0.59
Palmatine	0.29	352.40	40.80	-4.58	4	3.75
Reticuline	0.37	329.39	62.16	- 3.88	4	3.01
Stigmasterol	0.86	412.69	20.23	- 7.46	5	**8.56**
Syringin	0.53	372.37	**138.07**	- 1.03	7	**-1.31**
Tetrahydropalmatine	0.43	355.43	40.16	- 4.16	4	3.24

Two topological methods are used in SwissADME to predict the water solubility of the compounds. However, only the ESOL model, which establishes the linear relationship between log S and five molecular parameters namely the molecular weight, the number of rotatable bonds, the fraction of aromatic heavy atoms and Daylight's CLOGP is used. All predicted values are the decimal logarithm of the molar solubility in water, Log S [8]. Table 2 shows the SwissADME results of the thirteen compounds in terms of water solubility. The second column shows the classification of the compounds in terms of solubility based on the topological method that implements the ESOL model. Based on the prediction of SwissADME shown in Table 2, it can be inferred that syringin (12) is the most soluble one among the thirteen ligands.

Table 2. SwissADME Prediction of Water Solubility of the Target Metabolites of *Tinospora cordifolia*

Compound	Log S (ESOL)	Interpretation
20-Hydroxyecdysone	-2.78	soluble
β-sitosterol	- 7.90	poorly soluble
Berberine	- 4.55	moderately soluble
Columbamine	-4.37	moderately soluble
Columbin	-3.50	soluble
Jatrorrhizine	-4.37	moderately soluble
Magnoflorine	- 3.91	soluble
Menisperine	-4.12	moderately soluble
Palmatine	-4.58	moderately soluble
Reticuline	- 3.88	soluble
Stigmasterol	- 7.46	poorly soluble
Syringin	- 1.03	very soluble
Tetrahydropalmatine	-4.16	moderately soluble

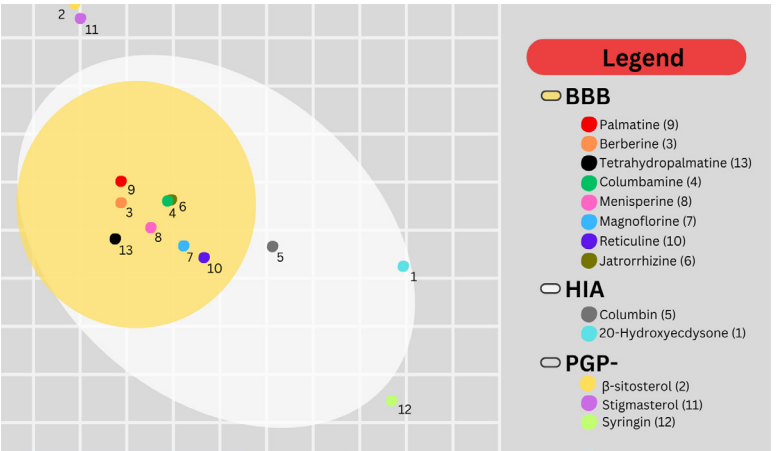

Figure 1. BOILED-Egg plot of the Selected Target Metabolites of *Tinospora cordifolia*

The passive human gastrointestinal absorption and blood-brain barrier permeation status of the compounds were all derived from the BOILED-Egg model of SwissADME (Figure 1). Among the thirteen compounds that were analyzed, berberine (3), columbamine (4), jatrorrhizine (6), magnoflorine (7), menisperine (8), palmatine (9), reticuline (10) and tetrahydropalmatine (13) were found to have high GI absorption. The same compounds were also found to successfully penetrate the BBB. Meanwhile, the next column shows the ability of the selected compounds to use P-glycoprotein (P-gp), an ATP binding cassette transporter that plays a significant role in drug absorption, distribution, and elimination. Generally, the P-gp acts as a transmembrane efflux pump that expels toxins and foreign substances out of cells, bringing about changes in the body [13]. At the beginning of drug discovery studies, it is crucial to determine whether a compound is a P-gp substrate as they are easily pumped out of the cell, thus, reducing their absorption. Among the thirteen compounds, only β-sitosterol (2), stigmasterol (11), and syringin (12) are not P-gp substrates [14]. Furthermore, the P-gp is expressed in different organs like the small intestine, blood vessels, blood-brain barrier, kidneys, and liver.

Table 3. SwissADME Prediction of Pharmacokinetics of the Target Metabolites of *Tinospora cordifolia*

Compound	GI Absorption	BBB permeant	P-gp substrate	Log Kp (cm/s)
20-Hydroxyecdysone	High	No	Yes	- 8.91
β-sitosterol	Low	No	No	- 2.20
Berberine	High	Yes	Yes	- 5.78
Columbamine	High	Yes	Yes	- 5.94
Columbin	High	No	Yes	- 6.95
Jatrorrhizine	High	Yes	Yes	- 5.94
Magnoflorine	High	Yes	Yes	- 6.44
Menisperine	High	Yes	Yes	- 6.30
Palmatine	High	Yes	Yes	- 5.79
Reticuline	High	Yes	Yes	- 6.17
Stigmasterol	Low	No	No	- 2.74
Syringin	Low	No	No	- 9.50
Tetrahydropalmatine	High	Yes	Yes	- 6.17

Table 4. SwissADME Prediction of CYP Inhibition of the Target Metabolites of *Tinospora cordifolia*

Compound	CYP1A2	CYP2C19	CYP2C9	CYP2D6	CYP3A4
20-Hydroxyecdysone	No	No	No	No	No
β-sitosterol	No	No	No	No	No
Berberine	Yes	No	No	Yes	Yes
Columbamine	Yes	No	No	Yes	Yes
Columbin	No	No	No	No	No
Jatrorrhizine	Yes	No	No	Yes	Yes
Magnoflorine	Yes	No	No	No	Yes
Menisperine	Yes	No	No	Yes	Yes
Palmatine	No	No	No	Yes	Yes
Reticuline	No	No	No	Yes	No
Stigmasterol	No	No	Yes	No	No
Syringin	No	No	No	No	No
Tetrahydropalmatine	No	No	No	Yes	Yes

In addition, the Log Kp which measures the ability of the skin to absorb a drug, or a chemical was also calculated. The more negative the value of Log Kp, the less likely the drug can permeate the skin membrane. β-sitosterol (2) has the least negative Log Kp, which means it has the highest skin permeability.

The Cytochrome P450 (CYP450) is a superfamily of isoenzymes that plays a major role in drug elimination through metabolic transformation process. The inhibition of CYP450 by a compound results in lower drug clearance and higher drug accumulation as the rate of enzyme-catalyzed reactions is reduced. It must be taken into consideration whether a drug is categorized as a CYP450 inhibitor to avoid increasing the potential for toxicity. Moreover, it was determined that about 80% of oxidative metabolism and around 50% of the overall elimination of most clinical drugs are attributable to the first three CYP families which include CYP1A2, CYP2C19, CYP2C9, CYP2D6, and CYP3A4 [15]. CYP inhibition prediction of the selected secondary metabolites (Table 4) showed that 20-Hydroxyecdysone (1), β-sitosterol (2), columbin (5) and syringin (12) do not inhibit any of these enzymes, which signifies that they are the least toxic compounds. Both berberine (3) and menisperine (8) displayed the greatest number of CYP enzymes inhibited, which means that among the thirteen selected compounds, they are the most toxic.

Lipinski's rule of five evaluates four key molecular properties associated with drug absorption and permeation. Particularly, it predicts poor absorption in compounds with more than 5 H-bond donors, 10-H bond acceptors, molecular weight of more than 500, and calculated MLOGP (Moriguchi octanol-water partition coefficient) of greater than 4.15 [16]. As indicated in Table 5, all compounds are orally active, while β-sitosterol (2) and stigmasterol (11) have violations mostly of the MLOGP and 20-hydroxyecdysone (1) on hydrogen bond donors (-NH or -OH). Furthermore, the Muegge rule makes use of a point filter is to identify compounds that are drug-like. There are four functional motifs in drug-like molecules that when combined to pharmacophore points, could help with hydrogen bonding to achieve drug interactions with targets [17].

Table 5. SwissADME Prediction of Druglikeness of the Target Metabolites of *Tinospora cordifolia*

Compound	Lipinski	Muegge
20-Hydroxyecdysone	Yes; 1 violation: NH or OH > 5	No; 1 violation: H-don > 5
β-sitosterol	Yes; 1 violation: MLOGP > 4.15	No; 2 violations: XLOGP3 > 5, Heteroatoms < 2
Berberine	Yes; 0 violation	Yes
Columbamine	Yes; 0 violation	Yes
Columbin	Yes; 0 violation	Yes
Jatrorrhizine	Yes; 0 violation	Yes
Magnoflorine	Yes; 0 violation	Yes
Menisperine	Yes; 0 violation	Yes
Palmatine	Yes; 0 violation	Yes
Reticuline	Yes; 0 violation	Yes
Stigmasterol	Yes; 1 violation MLOGP > 4.15	No; 2 violations: XLOGP3 > 5.
Syringin	Yes; 0 violation	Heteroatom < 2
Tetrahydropalmatine	Yes; 0 violation	Yes

To pass the filtering process, candidate drugs must receive two to seven pharmacophore points based on the functional group's amine, amide, alcohol, ketone, sulfone, sulfonamide, carboxylic acid, carbamate, guanidine, amidine, urea and ester. Referring to Table 5, all compounds, except 20-hydroxyecdysone (1), β-sitosterol (2), and stigmasterol (11) due to their violations in XLOGP3, heteroatoms, rotors, and hydrogen donors, contain pharmacophore points that could potentially provide key interactions with target proteins. Overall, the ligands berberine (3), columbamine (4), columbin (5), jatrorrhizine (6), magnoflorine (7), menisperine (8), palmatine (9), reticuline (10), syringin (12), and tetrahydropalmatine (13) consistently showed no violations to both Lipinski's and Muegge's criteria, indicating good drug-likeness. Lipinski's criteria primarily focus on the assessment of physicochemical properties related to the oral bioavailability of a drug, while Muegge's filter focuses on a more comprehensive and complementary set of rules emphasizing the balance between hydrogen bond donors and acceptors. In addition to using Lipinski's rule of five, the consistency of predictions with Muegge's filter enhances the reliability of pharmacokinetic properties of the compounds.

ProTox-II Prediction of the Target Metabolites. The analysis of 2D similarities and identification of toxic fragments in input compounds with determined median lethal doses (LD_{50}) are used as the basis for oral toxicity predictions [18]. The predicted toxicity classes shown in Table 6 depend on the respective LD_{50} values, based on the Globally Harmonized System of Classification and Labelling of Chemicals (GHS). Specifically, both Class 1, with LD_{50} values less than or equal to 5 mg/kg, and Class 2 compounds, with LD_{50} values from 6 to 50 mg/kg, are considered fatal if swallowed; Class 3 compounds with LD_{50} values from 51 to 300 mg/kg are toxic if swallowed; Class 4 compounds with LD_{50} values from 301 to 2000 mg/kg are harmful if swallowed; Class 5 compounds with LD_{50} values from 2001 to 5000 mg/kg may be harmful if swallowed; and Class 6 compounds with LD_{50} values greater than 5000 mg/kg are generally considered non- toxic. Table 6 shows that 20-hydroxyecdysone (1) is the only Class 6 compound predicted to be orally non-toxic.

Table 6. ProTox-II Prediction of Acute Oral Toxicity and Toxicity of the Target Metabolites of *Tinospora cordifolia*

Compound	Predicted LD_{50}	Predicted Toxicity Class	Hepatotoxicity	Carcinogenicity	Immunotoxicity	Mutagenicity	Cytotoxicity
20-Hydroxyecdysone	9000 mg/kg	6	Inactive (0.74)	**Active** (0.78)	**Active** (0.93)	Inactive (0.74)	Inactive (0.76)
β-sitosterol	890 mg/kg	4	Inactive (0.87)	Inactive (0.60)	**Active** (0.99)	Inactive (0.98)	Inactive (0.94)
Berberine	200 mg/kg	3	Inactive (0.82)	Below Threshold (0.56)	**Active** (0.99)	Below Threshold (0.62)	**Active** (0.96)
Columbamine	200 mg/kg	3	Inactive (0.79)	Inactive (0.53)	**Active** (0.98)	Below Threshold (0.55)	Inactive (0.50)
Columbin	555 mg/kg	4	Inactive (0.85)	Inactive (0.62)	**Active** (0.98)	Inactive (0.79)	Inactive (0.53)
Jatrorrhizine	200 mg/kg	3	Inactive (0.81)	Inactive (0.54)	**Active** (0.98)	Below Threshold (0.52)	Inactive (0.51)
Magnoflorine	401 mg/kg	4	Inactive (0.96)	Inactive (0.64)	**Active** (0.94)	Inactive (0.59)	Inactive (0.69)
Menisperine	350 mg/kg	4	Inactive (0.96)	Inactive (0.64)	**Active** (0.98)	Inactive (0.58)	Inactive (0.66)
Palmatine	200 mg/kg	3	Inactive (0.77)	Below Threshold (0.50)	**Active** (0.96)	**Active** (0.57)	**Active** (0.56)
Reticuline	700 mg/kg	4	Inactive (0.94)	Inactive (0.63)	**Active** (0.92)	Inactive (0.50)	Inactive (0.51)
Stigmasterol	890 mg/kg	4	Inactive (0.87)	Inactive (0.60)	**Active** (0.99)	Inactive (0.98)	Inactive (0.94)
Syringin	4000 mg/kg	5	Inactive (0.83)	Inactive (0.85)	**Active** (0.92)	Inactive (0.80)	Inactive (0.76)
Tetrahydropalmatine	580 mg/kg	4	Inactive (0.95)	Inactive (0.55)	**Active** (0.76)	Inactive (0.55)	Inactive (0.50)

This is followed by the Class 5 compound, syringin (12); then the Class 4 compounds, β-sitosterol (2), columbin (5), magnoflorine (7), menisperine (8), reticuline (12), stigmasterol (11), and tetrahydropalmatine (13), in terms of toxicity severity. Moreover, berberine (3), columbamine (4), jatrorrhizine (6), and palmatine (9) were shown to be the most orally toxic compounds in the group, since these were classified as Class 3 compounds.

Oleaga et al. (2016) defined organ toxicity as characterized by any detrimental change in the physiology, biochemistry, or morphology of an organ, caused by toxicants acting either directly or indirectly through disrupting normal physiological mechanisms [19]. This includes hepatotoxicity, nephrotoxicity, neurotoxicity, and more. In particular, the ProTox-II platform utilizes hepatotoxicity as its only model under this classification [20]. As seen in Table 6, all compounds are predicted to be non-hepatotoxic, which means that they are not capable of causing drug-induced liver injury. For toxicological endpoints, the ProTox-II server utilizes four models under this toxicity classification, particularly carcinogenicity, immunotoxicity, mutagenicity, and cytotoxicity [20]. Table 6 also shows that 20-hydroxyecdysone (1) and palmatine (9) are the only compounds predicted to be carcinogenic and mutagenic, respectively. Likewise, berberine (3) and palmatine (9) are the only ones considered to be cytotoxic, while all thirteen compounds are found to be immunotoxic. Furthermore, those that were classified below threshold had lower confidence values than the perceived ranges and were, therefore, omitted.

However, based on several literature proving the anti-inflammatory effects of *Tinospora cordifolia*, the extract has shown no significant toxicities. In a study by Philip et al. (2018), for the acute oral toxicity of *Tinospora cordifolia* chloroform extract at a high dose, 2000 mg/kg body weight, the rats showed no significant signs of toxicity and mortality. The liver and serum analyses also showed no significant toxicological changes [7].

Table 7. Key Residues of Ligands with Optimal Binding Energies

Protein (PDB ID)	Ligands	Binding Energy (kcal/mol)	Key Residues of Interaction
MMP-13 (P45452)	Stigmasterol	-9.8	Phe107, Phe189, Pro191, Pro193, Tyr104, Tyr176, Tyr195, Val106
MMP-2 (P08253)	Berberine	-8.9	Asn245, Cys363, Glu243, Pro391, Ser246, Thr250
MMP-19 (Q99542)	20-Hydroxye-cdysone	-8.9	Arg103, Arg301, Gln347, Leu101, Leu298, Pro344, Pro387
COX-1 (P00395)	β-sitosterol	-8.8	Ala24, Leu21, Leu20, Phe393, Trp6
LT-β (Q06643)	β-sitosterol	-8.8	Ala166, Gly173, Leu102, Pro175, Pro226, Tyr220
Nf-kb1 (P19838)	Stigmasterol	-8.6	Arg934, Leu581
5-LOX (P09917)	Columbin	-8.5	Ala454, Arg 247, Arg371, Ile366, Leu245, Val244
15-LOX (P16050)	β-sitosterol	-8.4	Arg394, Leu167, Phe77, Tyr97, Tyr395
MMP-1 (P03956)	Columbin	-8.3	Glu311, Leu314, Pro310, Val312
MMP-8 (P22894)	Columbin	-8.2	Ala132, Asp135, Leu139, Phe212, Val142
NIK (Q99558)	β-sitosterol	-8.2	Cys605, Gln784, Leu777, Phe778, Phe858, Tyr857
	Stigmasterol	-8.2	Cys605, Leu777, Phe778, Pro855, Tyr857
IL-17A (Q16552)	Stigmasterol	-8.2	Trp51, Tyr43, Tyr44, and Trp67
TGF-β (P01137)	Stigmasterol	-8.1	Glu99, Leu64, Trp30, Trp32

Another study by Badar et al. (2005) where *Tinospora cordifolia* extract was administered to patients with allergic rhinitis, 83% of the participants had total relief from sneezing, 69% showed a 100% improvement in the case of nasal discharge, nasal obstruction was totally cleared in 61% of the participants, and a 100% improvement was also observed in 71% of the patients for nasal pruritus. The study also reported that *Tinospora cordifolia* is well tolerated because out of the 36 patients who took the extract, only two reported nasal pain and one for headache, which were all relieved by analgesics [21].

As opposed to the results generated from Protox-II, the absence of significant adverse effects and toxicities from these studies can prove the safety of *Tinospora cordifolia*. These compounds present in the extract may have synergistic effects that, when metabolized after oral administration, may lead to less toxicity compared to the program results. It is notable that Protox-II is merely used as a tool for the prediction of numerous toxicity endpoints, and should not limit the anti-inflammatory potential of the secondary metabolites.

Molecular Docking. The results of docking for each protein-ligand complex revealed twenty poses arranged based on their docking scores or binding energy (kcal/mol) from lowest to highest, with the lowest or most negative being the most optimal. Pose generation requires scoring functions to enhance the quality and identification of correct bioactive conformation of a ligand in a receptor [22]. These scoring functions roughly represent and estimate binding affinity in relation to intermolecular interactions that strengthen the protein-ligand complex, while considering the energy being used. This binding energy is released as a ligand molecule interacts with a target protein, reducing the total energy of the complex, referred to as the Gibbs free energy (ΔG) [23]. A low docking score indicates that less energy is used to stabilize the binding, thus, the more negative the score of a conformation, the stronger it is.

The most negative score, which corresponds to the most ideal ligand pose, is selected for each set of ligand and protein. Since a starting value of -6.0 kcal/mol is generally considered for standard drugs with small molecular structures [24], only top-ranked scores that are lower than -8.0 kcal/mol were considered in this study, in consideration of the large structural size of the complexes. Table 7 shows the protein-ligand pairs with their binding affinities in descending order.

Among them, stigmasterol (11) exhibited the lowest binding energy of -9.8 kcal/mol when docked to MMP-13 (Table 7). Stigmasterol (11) was also revealed to have good binding affinities with four other receptors: Nf-kb1 (- 8.6 kcal/mol), NIK and IL-17A (-8.2 kcal/mol), and TGF-β (-8.1 kcal/mol), that are all stronger than that of the comparator drug.

Following stigmasterol (11), berberine (3) and 20-hydroxyecdysone (1) are bound with MMP-2 and MMP-19, respectively, at -8.9 kcal/mol. Meanwhile, β-sitosterol (2) exhibited -8.8 kcal/mol with both COX-1 and LT-B -8.4 kcal/mol with 15-LOX, and -8.2 kcal/mol with NIK. Columbin (5) revealed a binding affinity of -8.5 kcal/mol with 5-LOX, -8.3 kcal/mol with MMP-1, and -8.2 kcal/mol with MMP-8.

Positive Controls. The novelty of some proteins as anti-inflammatory targets limits the comparator compounds available as positive controls versus the ligands in this study. The binding energy exhibited by the interactions between the following ligands with the proteins was compared to that of an available positive control with the protein, respectively: stigmasterol with MMP-13, β-sitosterol with COX-1, stigmasterol with Nf-κb1(p50), columbin with 5-LOX, and β-sitosterol and stigmasterol with NIK.

Stigmasterol on MMP-13, Nf-κb1(p50), NIK, IL-17A, and TGF- β. Figure 2a shows the interactions predicted to be formed by stigmasterol (11) with MMP-13. Stigmasterol (11) with MMP-13 revealed the most negative binding energy of -9.8 kcal/mol and therefore the strongest affinity and most stable conformation among other compounds. Three carbon hydrogen bond interactions were predicted at Tyr104, Pro193, and Pro191 residues, while a lone *pi-pi* T-shaped interaction was formed by Phe107 with the aromatic ring of stigmasterol. Multiple alkyl and *pi*-alkyl interactions are also predicted at Tyr176, Phe189, Tyr195, and Val106 residues of MMP-13.

There are several studies on MMP-13, an important metalloproteinase mediator in inflammation, including its mechanisms in inflammatory bowel disease. Vandenbroucke et al. (2013) suggest that it is a potential target in treating TNF-dependent intestinal barrier inflammation, in which its inhibition decreases TNF levels that are primarily elevated in such cases [25]. However, no compound targeting MMP-13 specifically for anti-inflammation has been identified thus far aside from batimastat for antiangiogenesis. Batimastat, a broad-spectrum MMP inhibitor used as an antiangiogenic agent, exhibited an energy of -7.3 kcal/mol upon binding to MMP-13, which is inferior compared to the resultant binding energy between stigmasterol (11) and MMP-13. Though stigmasterol (11) showed a stronger affinity than batimastat, the difference in their binding sites to the same MMP must be highly considered.

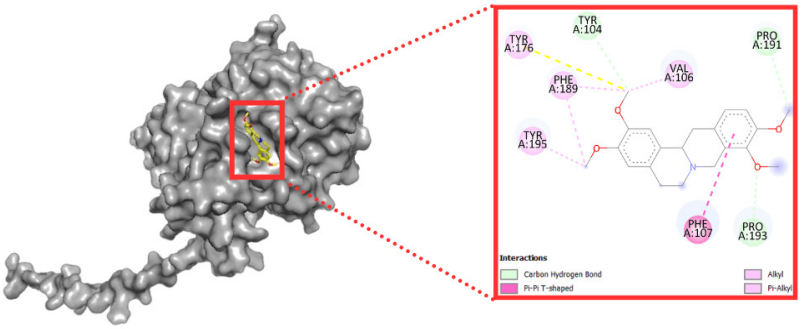

Figure 2a. Ligand Interactions of Stigmasterol with MMP-13

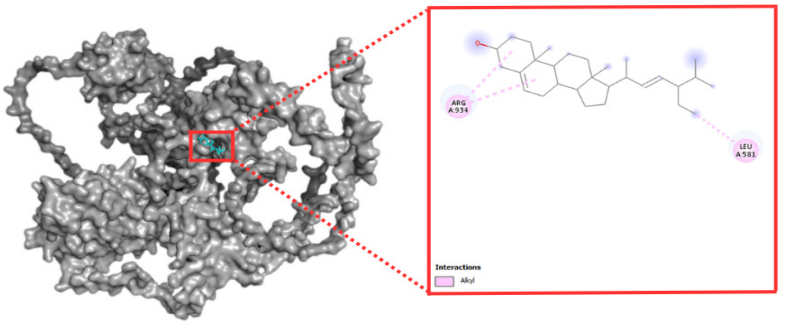

Figure 2b. Ligand Interactions of Stigmasterol with Nf-κb1 (p50)

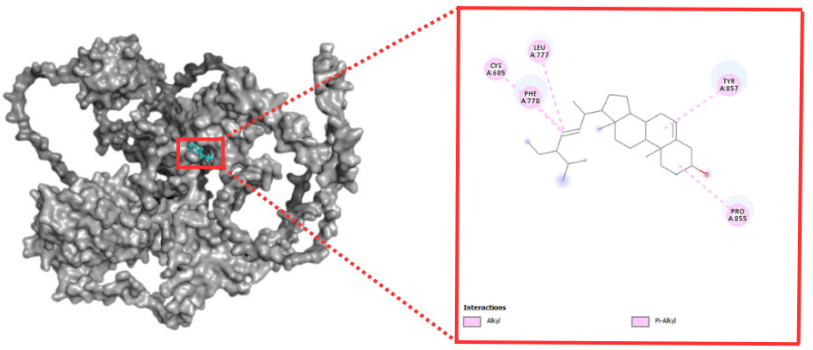

Figure 2c. Ligand Interactions of Stigmasterol with NIK

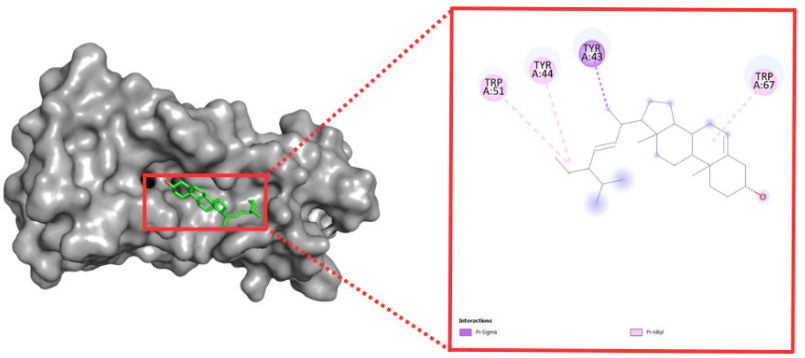

Figure 2d. Ligand Interactions of Stigmasterol with IL-17A

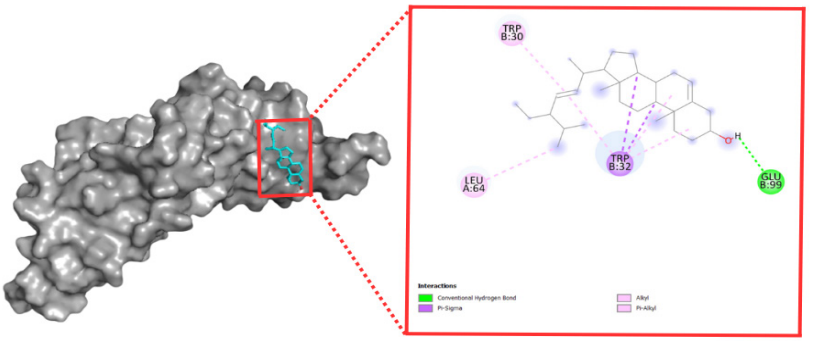

Figure 2e. Ligand Interactions of Stigmasterol with TGF-β

Moving to Nf-κb1(p50) which is a part of the canonical signaling pathway of the Nf-κb that serves as a critical mediator for inflammatory responses [26]. Its activation happens via proinflammatory cytokines such as interleukin-1 (IL-1) and tumor necrosis factor (TNFα) which in turn activates RelA that functions in the expression of proinflammatory and cell survival genes [27]. Stigmasterol (11) demonstrated a binding energy at -8.6 kcal/mol, forming alkyl interactions at Arg934 and Leu581 residues (Figure 2b). Dexamethasone, a widely used anti-inflammatory corticosteroid by Nf-κb inhibition was also docked to Nf-κb1(p50) with a binding energy of -7.2 kcal/mol, notably higher than that of stigmasterol (11), but on different binding sites.

Moreover, NIK with stigmasterol (11) (Figure 2c) yielded a binding affinity of -8.2 kcal/mol. Alkyl interactions are formed by stigmasterol (11) at Pro855, Tyr857 and Phe778. Pi-alkyl interactions at Cys605 and Leu777 are also predicted. Staurosporine, a natural antibiotic isolated from *Streptomyces staurosporeus*, with a potent kinase inhibitory activity that was found to inhibit NIK exhibited a binding energy of -8.0 kcal/mol upon docking with NIK, a value not far from that exhibited by stigmasterol (11) with the same receptor.

In the case of IL-17A with stigmasterol (11) (Figure 2d), a binding affinity of -8.1 kcal/mol was shown. *Pi*-sigma and *pi*-alkyl interactions are predicted to form at Trp51, Tyr43, Tyr44, and Trp67 residues. IL-17A induces gene expression of proinflammatory cytokines TNF, IL-1, IL-6, G-CSF, and GM-CSF, chemokines CXCL1, CXCL5, IL-8, CCL2, and CCL7, antimicrobial peptides defensins and S100 proteins, and matrix metalloproteinases MMP1, MMP3, and MMP13. It is also involved in neutrophil recruitment to inflammatory sites [28].

Meanwhile, TGF-β with stigmasterol (Figure 2e) yielded a binding affinity of -8 kcal/mol. Figure 2e revealed that Trp30 and Trp32 formed pi-alkyl and pi-sigma interactions with stigmasterol (11), respectively, while Leu64 formed alkyl interactions and Glu99 formed conventional hydrogen bond interactions. As an anti-inflammatory factor, TGF-β has been demonstrated to suppress the generation and activity of effector T cells and antigen-presenting dendritic cells. Moreover, it can modulate natural killer cells, macrophages, dendritic cells, and granulocytes, thus reducing inflammation [29].

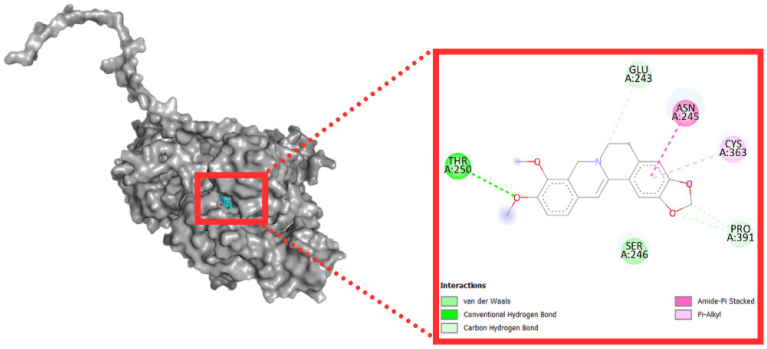

Figure 3a. Ligand Interactions of Berberine with MMP-2

Berberine on MMP-2. MMP-2 with berberine (3) showed a low binding affinity of -8.9 kcal/mol by different interactions (Figure 3a). A van der Waals interaction is predicted to form at the Ser246 residue, with another conventional hydrogen bond at Thr250. Pro391 and Glu243 residues interact with the berberine (3) structure by carbon hydrogen bonding. An amide-pi stacked interaction is predicted between MMP-2 and berberine (3) at Asn245 residue, while there is a pi-alkyl bond predicted at Cys363 of MMP-2. As a member of the MMP family, MMP-2 contributes to the inflammatory response by controlling the activity of pro-inflammatory cytokines and chemokines [30]. Specifically, it allows the recruitment and movement of inflammatory cells by breaking down extracellular matrices [31].

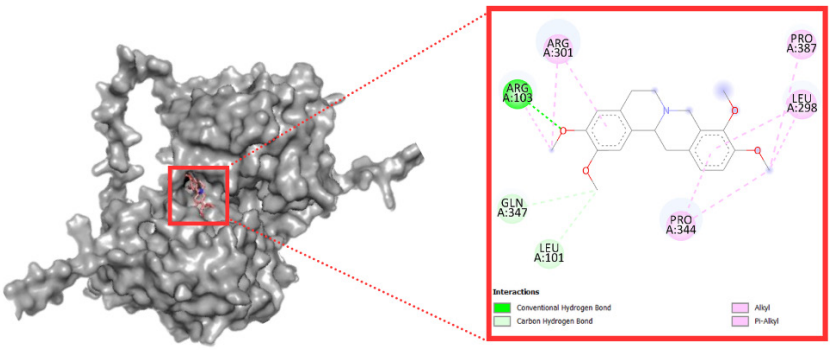

Figure 4a. Ligand Interactions of 20-Hydroxyecdysone with MMP-19

20-Hydroxyecdysone on MMP-19. MMP-19 with 20-hydroxyecdysone (1) (Figure 4a) interacts at -8.9 kcal/mol. 20-hydroxyecdysone (1) is predicted to form a conventional hydrogen bond with MMP-19 at Arg103, and two carbon hydrogen bonds at Gln347 and Leu101. Leu298, Pro344, and Arg301 residues are predicted to form a pi-alkyl interaction with the aromatic rings of 20-hydroxyecdysone (1), while Arg103, Arg301, Pro344, Pro387, and Leu298 are all predicted to form alkyl interactions. MMP-19 contributes to the inflammation of lungs by enhancing the Th2-driven eosinophilia and airway hyperactivity [30]. Its significance lies in its capacity to regulate the accumulation of tenascin-C, a Th2-cell related inflammatory lung response, by cleaving it like collagen and other matrix components in the lungs [32].

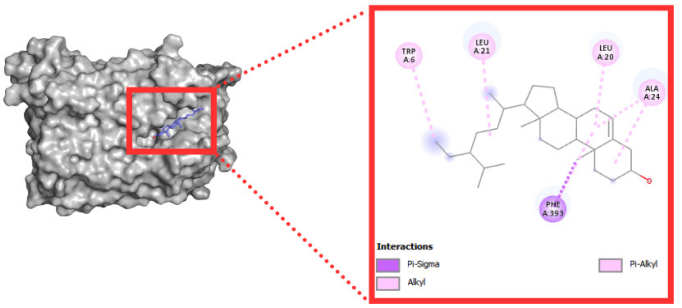

Figure 5a. Ligand Interactions of β-sitosterol with COX-1

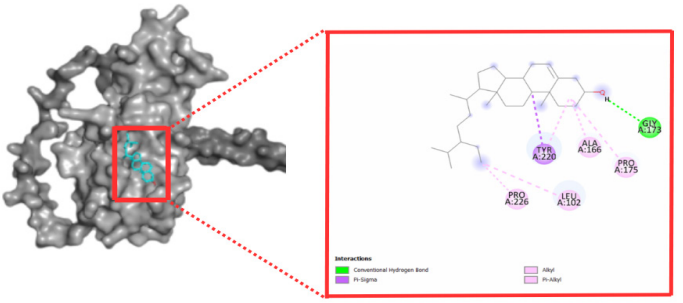

Figure 5b. Ligand Interactions of β-sitosterol with LT-β

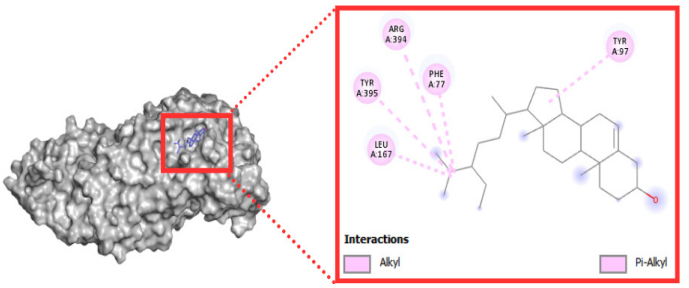

Figure 5c. Ligand interactions of β-sitosterol with 15-LOX

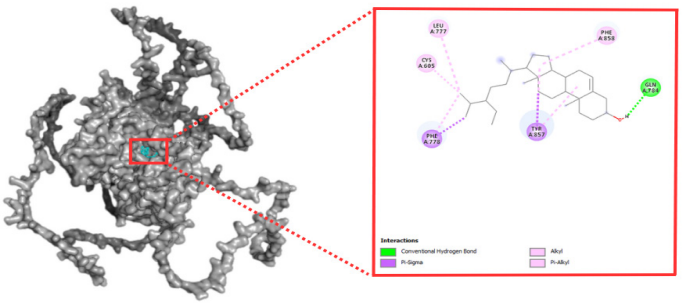

Figure 5d. Ligand Interactions of β-sitosterol with NIK

β-sitosterol on COX-1, LT-β, 15-LOX, and NIK. β-sitosterol (2) and COX-1 (Figure 5a) showed a low binding affinity of -8.8 kcal/mol wherein *pi*-sigma, alkyl, and *pi*-alkyl bonds interactions at binding sites were predicted, specifically at the Phe393, Trp6, Leu21, Leu20, and Ala24 residues of COX-1, respectively. However, the binding energy of selective COX-1 inhibitor Ketoprofen was found to be superior at -11.2 kcal/mol [33]. The COX pathway plays a crucial role in the initiation of inflammation due to its association in the production of prostaglandins. Particularly, COX-1 is involved in the aggregation of platelets, regulation of kidney arteriole vasodilation, and protection of the innermost mucosa of the gastrointestinal tract [34].

Moreover, β-sitosterol (2) with LT-β has yielded a binding affinity of -8.8 kcal/mol wherein on *Pi*-alkyl bonds were predicted at Ala166 and Pro175 while alkyl bonds at Pro226, and Leu102 were also predicted to form as shown on Figure 5b.

Pi-sigma and conventional hydrogen bond interactions are also predicted to form at Tyr220 and Gly173, respectively. LT-β contributes to the regulation of immune responses as it is essential for the development of secondary lymphoid tissues [35].

Furthermore, based on Figure 5c, it shows that 15-LOX with β-sitosterol (2) binds at -8.4 kcal/mol, with its interactions primarily alkyl and *pi*-alkyl. Tyr97 residue is predicted to form an interaction with the heterocyclic ring of β-sitosterol (2). The compound binds to 15-LOX at Leu167, Tyr395, Arg394, and Phe77 residues. 15-LOX is a dioxygenase involved in the peroxidation of polyunsaturated fatty acids (PUFAs) into their hydroxyperoxy derivatives, which include specialized inflammatory mediators, highlighting the involvement of this pathway in the inflammatory response [36].

Meanwhile, NIK with β-sitosterol (2) (Figure 5d), interacts with a binding affinity of -8.2 kcal/mol. A conventional hydrogen bond is predicted to form at Gln784 residue. Moreover, a *pi*-sigma interaction at Phe778 and Tyr857, a pi-alkyl interaction at Leu777 and Cys605, and an alkyl interaction at Phe858 are also predicted to form.

Columbin on 5-LOX, MMP-1, and MMP-8. Columbin (5), when docked to 5-LOX (Figure 6a), yielded a binding affinity of -8.5 kcal/mol which is lower compared to Setileuton, a novel selective 5-LOX inhibitor, with a docking score of -9.6 kcal/mol [37]. During inflammation, particularly in asthma, the 5-LOX pathway gives rise to proinflammatory leukotrienes (LTs) which are targets of LT antagonists to reduce inflammation [38].

Moreover, the docking analysis of MMP-1 with columbin (5), as shown on Figure 6b, revealed a binding affinity of -8.3 kcal/mol, with conventional hydrogen bond reactions at Val312, Glu311, and Leu314 residues. Pro310 residue of MMP-1 interacts with columbin (5) by a carbon hydrogen bond and a *pi*-sigma with its aromatic ring. On the other hand, the docking results of columbin (5) with MMP-8 displayed a binding affinity of -8.2 kcal/mol as shown on Figure 6c. It is predicted to have an interaction with a single carbon hydrogen bond at Asp135, while the rest are alkyl and *pi*-alkyl bonds between MMP-8 and columbin (5) at Val142, Leu139, Phe212, and Ala132 residues.

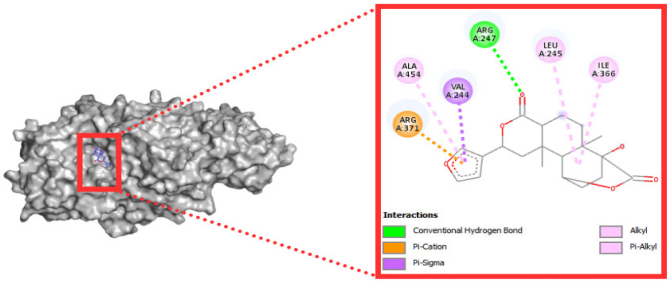

Figure 6a. Ligand Interactions of Columbin with 5-LOX

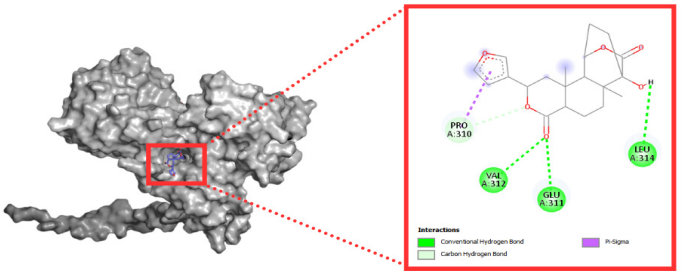

Figure 6b. Ligand Interactions of Columbin with MMP-1

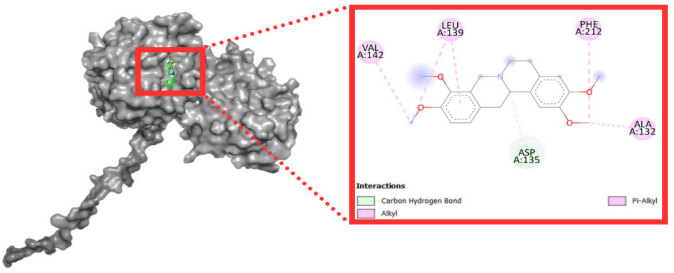

Figure 6c. Ligand Interactions of Columbin with MMP-8

From all the compounds docked with considerable docking scores, the interaction between MMP-13 and stigmasterol (11) has the lowest binding affinity of -9.8 kcal/mol. On the other hand, the interaction between TGF-β and stigmasterol (11) has the highest binding affinity of -8.1 kcal/mol. Most of the docked interactions involved in the binding are *pi*-alkyl and alkyl bonds which are found to contribute to the binding interaction of the ligands and proteins. Other interactions like *pi*-stigma, conventional hydrogen bond, carbon hydrogen bonds, *pi-pi* T-shaped, Van der Waals, and *pi*-cations also contributed to the stabilization of the binding structures. Stronger van de Waals interactions result in higher binding affinities and most high-affinity ligands require strong H-bonds [39]. In addition, in a study by Chen et al. (2016), protein-ligand affinity depends on the effects of H-bond pairing on free energy change. All strong-strong H-bond pairings increase the ligand binding affinity.

However, weak-weak H-bonding tends to be more favorable in increasing ligand binding affinity than strong-weak H-bonds, which implies that it may be inaccurate to generalize that H-bonds do not significantly affect binding affinity [40]. However, the conventional hydrogen bonds and van der Waals interactions were found to contribute greatly specifically only to the binding structure to the targets of columbin (5) with MMP-1 and berberine (3) with MMP-2, respectively.

The docked metabolites of *Tinospora cordifolia* to essential proteins show they can be potential lead candidates for treating different inflammatory diseases. Upon performing molecular docking, 14 conformations showed ideal binding affinity, with Stigmasterol (11) being the preeminent metabolite as it displayed the most significant number of desirable binding affinities among the chosen ligands. Regarding the toxicities of the secondary metabolites, ProTox-II revealed that all compounds are predicted to be immunotoxic. However, based on several literatures proving the anti-inflammatory effects of *Tinospora cordifolia*, as an extract, has shown no significant toxicities and it is notable that Protox-II is merely used as a tool for the prediction of numerous toxicity endpoints, and should not limit the anti-inflammatory potential of the secondary metabolites. Hence, the results generated from this *in silico* study could commence drug therapy discoveries when further supplemented by in vitro and in vivo experiments. Based on the results of the present study, several compounds from *Tinospora cordifolia* interact well with the target proteins and could mean promising candidates as new anti-inflammatory agents.

Conclusion

The docking and analyses of *Tinospora cordifolia* metabolites to key proteins in inflammatory pathways revealed potential lead candidates, namely, 20-Hydroexyecdysone (1), β-sitosterol (2), Berberine (3), Columbin (5), and Stigmasterol (11). However, while these 5 secondary metabolites have promising binding activity, their potential as anti-inflammatory leads are limited by their predicted toxicity based on ProTox-II *in silico* studies. Hence, further investigation regarding these secondary metabolites of *Tinospora cordifolia* is necessary for prospective drug discovery and design applied to inflammatory pathways. The major findings of this study showed great potential for the development of a systematic approach to drug design targeting inflammatory diseases, which could be explored in future research on *Tinospora cordifolia*.

Acknowledgments

The authors would like to express their sincerest gratitude to the Faculty of Pharmacy, University of Santo Tomas, Manila, Philippines.

Conflict of Interest

The authors declare no conflict of interest.

Author Contributions

YHRA, CPA, BNFA, MEVA, VRRB, GARB, ARLB, LJPB, JACC, AEC, MSAE, and ALC made equal contributions to the conceptualization and methodology of the entire manuscript; Data collection YHRA, CPA, BNFA, MEVA, ARLB, LJPB, JACC, and AEC; Interpretation and analysis of data, YHRA, CPA, BNFA, MEVA, VRRB, GARB, ARLB, LJPB, JACC, AEC, MSAE and ALC; original draft preparation, YHRA, CPA, BNFA, MEVA, VRRB, GARB, ARLB, LJPB, JACC, AEC; review and editing MSAE and ALC. All authors have read and agreed to the final version of the manuscript.

Funding

None.

Institutional Review Board Statement

Not applicable.

Informed Consent Statement

Not applicable.

References

[1] Pahwa, R., Goyal, A., & Jialal, I. (2022). Chronic inflammation. In: StatPearls. StatPearls Publishing. Retrieved September 21,2022 from https://www.ncbi.nlm.nih.gov/books/NBK4 93173/

[2] Deng, W., Du, H., Liu, D., & Ma, Z. (2022). Editorial: The role of natural products in chronic inflammation. Frontiers inPharmacology,13. https://doi.org/10.3389/fphar.2022.901538

[3] Saha, S., & Ghosh, S. (2012). Tinospora cordifolia: One plant, many roles. Ancient science of life, 31(4), 151.

[4] Ghatpande, N. S., Misar, A. V., Waghole, R. J., Jadhav, S. H., & Kulkarni, P. P. (2019). Tinospora cordifolia protects against inflammation associated anemia by modulating inflammatory cytokines and hepcidin expression in male Wistar rats. Scientific Reports, 910969.https://doi.org/10.1038/s41598-019-47458-0

[5] Sumanlata, Akanksha Suman, & Rajeev Sharma. (2019). Evaluation of Anti- Inflammatory and Antipyretic Effect of Aqueous Extract of Tinospora Cordifolia in Rats. International Journal of Research, 6(8), 340–346.

[6] Jacob J., & B. K. Prakash. (2015). Dual COX/LOX inhibition: screening and evaluation of effect of medicinal plants of Kerala as Antiinflammatory agents. Journal of Pharmacognosy and Phytochemistry, 3(6), 62–66.

[7] Philip, S., Tom, G., & Vasumathi, A. V. (2018). Evaluation of the anti-inflammatory activity of Tinospora cordifolia (Willd.) Miers chloroform extract - a preclinical study. Journal of Pharmacy and Pharmacology, 70(8), 1113–1125. https://doi.org/10.1111/jphp.12932

[8] Daina, A., Michielin, O., & Zoete, V. (2017). SwissADME: a free web tool to evaluate pharmacokinetics, drug-likeness and medicinal chemistry friendliness of small molecules. Scientific Reports, 7(1). https://doi.org/10.1038/srep42717

[9] Singh, V. (2020). Structure based Docking of Secondary Metabolites against DrpE1 to Treat Tuberculosis. International Journal for Research in Applied Science and Engineering Technology, 8(6), 2515–2520. https://doi.org/10.22214/ijraset.2020.6405

[10] Quimque, M. T. J., Notarte, K. I. R., Fernandez, R. A. T., Mendoza, M. A. O., Liman, R. A. D., Lim, J. A. K., Pilapil, L. A. E., Ong, J. K. H., Pastrana, A. M., Khan, A., Wei, D.-Q., & Macabeo, A. P. G. (2021). Virtual screening-driven drug discovery of SARS-CoV2 enzyme inhibitors targeting viral attachment, replication, post- translational modification and host immunity evasion infection mechanisms. Journal of Biomolecular Structure and Dynamics, 39(12), 4316–4333. https://doi.org/10.1080/07391102.2020.1776 639

[11] Ritchie, T. J., & Macdonald, S. J. (2009). The impact of aromatic ring count on compound developability – are too many aromatic rings a liability in drug design? Drug Discovery Today, 14(21–22), 1011–1020. https://doi.org/10.1016/j.drudis.2009.07.014

[12] Waring, M. J. (2010). Lipophilicity in drug discovery. Expert Opinion on Drug Discovery,5(3), 235–248. ttps://doi.org/10.1517/17460441003605098

[13] Lin, J. H., & Yamazaki, M. (2003). Role of P-glycoprotein in pharmacokinetics: clinical implications. Clinical pharmacokinetics, 42(1), 59–98. https://doi.org/10.2165/00003088-200342010-00003

[14] Wang, P. H., Tu, Y. S., & Tseng, Y. J. (2019). PgpRules: A decision tree based prediction server for P-glycoprotein substrates and inhibitors. Bioinformatics, 35(20), 4193–4195. https://doi.org/10.1093/bioinformatics/btz213

[15] Zhao, M., Ma, J., Li, M., Zhang, Y., Jiang, B., Zhao, X., Huai, C., Shen, L., Zhang, N., He, L., & Qin, S. (2021). Cytochrome P450 Enzymes and Drug Metabolism in Humans. International journal of molecular sciences, 22(23), 12808. https://doi.org/10.3390/ijms222312808

[16] Lipinski, C. A., Lombardo, F., Dominy, B. W., & Feeney, P. J. (2001). Experimental and computational approaches to estimate solubility and permeability in drug discovery and development settings 1PII of original article: S0169-409X(96)00423-1. The article was originally published in Advanced Drug Delivery Reviews 23 (1997) 3–25. 1. Advanced Drug Delivery Reviews, 46(1–3), 3–26. https://doi.org/10.1016/s0169- 409x(00)00129-0

[17] Muegge, I., Heald, S. L., & Brittelli, D. (2001). Simple Selection Criteria for Drug- like Chemical Matter. Journal of Medicinal Chemistry, 44(12), 1841–1846. https://doi.org/10.1021/jm015507e

[18] Drwal, M. N., Banerjee, P., Dunkel, M., Wettig, M. R., & De Braud, F. (2014). ProTox: a web server for the in silico prediction of rodent oral toxicity. Nucleic Acids Research, 42(W1), W53–W58. https://doi.org/10.1093/nar/gku401

[19] Oleaga, C., Bernabini, C., Smith, A. S. T., Srinivasan, B., Jackson, M., McLamb, W., Platt, V., Bridges, R., Cai, Y., Santhanam, N., Berry, B., Najjar, S., Akanda, N., Guo, X., Martin, C., Ekman, G., Esch, M. B., Langer, J., Ouedraogo, G., Hickman, J. J. (2016). Multi-organ toxicity demonstration in a functional human in vitro system composed of four organs. Scientific Reports, 6(1). https://doi.org/10.1038/srep20030

[20] Banerjee, P., Eckert, A., Schrey, A. K., & De Braud, F. (2018). ProTox-II: a webserver for the prediction of toxicity of chemicals. Nucleic Acids Research, 46(W1),W257–W263. https://doi.org/10.1093/nar/gky318

[21] Badar, V. A., Thawani, V. R., Wakode, P. T., Shrivastava, M. P., Gharpure, K. J., Hingorani, L. L., & Khiyani, R. M. (2005). Efficacy of Tinospora cordifolia in allergic rhinitis. Journal of ethnopharmacology, 96(3), 445-449.

[22] Pantsar, T. & Poso, A. (2018). Binding affinity via docking: Fact and fiction. Molecules, 23(8),1899. https://doi.org/10.3390/molecules23081899

[23] Alos, H. C., Billones, J. B., Vasquez, R. D., & Castillo, A. L. (2019). Antiangiogenesis potential of alpinumisoflavone as an inhibitor of matrix metalloproteinase-9 (MMP-9) and vascular endothelial growth factor receptor-2 (VEGFR-2). Current Enzyme Inhibition, 15(3),159-178. https://doi.org/10.2174/15734080166662001 23160509

[24] Nath, A., Kumer, A., Zaben, F., & Khan, M. W. (2021). Investigating the binding affinity, molecular dynamics, and ADMET properties of 2,3-dihydrobenzofuran derivatives as an inhibitor of fungi, bacteria, and virus

[25] Vandenbroucke, R. E., Dejonckheere, E., Van Hauwermeiren, F., Lodens, S., De Rycke, R., Van Wonterghem, E., Staes, A., Gevaert, K., López□Otin, C., & Libert, C. (2013). Matrix metalloproteinase 13 modulates intestinal epithelial barrier integrity in inflammatory diseases by activating TNF. EMBO Molecular Medicine, 5(7), 1000–1016. https://doi.org/10.1002/emmm.201202100

[26] Yu, H., Lin, L., Zhang, Z., Zhang, H., & Hu, H. (2020). Targeting NF-κB pathway for the therapy of diseases: mechanism and clinical study. Signal Transduction and Targeted Therapy, 5(1), 1-23.

[27] Lawrence, T. (2009). The nuclear factor NF-κB pathway in inflammation. Cold Spring Harbor Perspectives in Biology, 1(6).

[28] Iwakura, Y., Ishigame, H., Saijo, S., & Nakae, S. (2011). Functional Specialization of Interleukin-17 Family Members. Immunity, 34(2), 149–162. https://doi.org/10.1016/j.immuni.2011.02.012

[29] Liu, Z.-wei, Zhang, Y.-ming, Zhang, L.-ying, Zhou, T., Li, Y.-yang, Zhou, G.-cheng, Miao, Z.-ming, Shang, M., He, J.-peng, Ding, N.-, & Liu, Y.-qi. (2022). Duality of interactions between TGF-β and TNF-α during tumor formation. Frontiers in Immunology, 12. https://doi.org/10.3389/fimmu.2021.810286

[30] Nissinen, L., & Kähäri, V. M. (2014). Matrix metalloproteinases in inflammation. Biochimica et Biophysica Acta - General Subjects, 1840(8), 2571–2580. https://doi.org/10.1016/j.bbagen.2014.03.007

[31] Mori, S., Pawankar, R., Ozu, C., Nonaka, M., Yagi, T., & Okubo, K. (2012). Expression and roles of MMP-2, MMP-9, MMP-13, TIMP-1, and TIMP-2 in allergic nasal mucosa. Allergy, Asthma and Immunology Research, 4(4), 231–239. https://doi.org/10.4168/aair.2012.4.4.231

[32] Gueders, M. M., Stuart John Hirst, Quesada-Calvo, F., Paulissen, G., Hacha, J., Gilles, C., Gosset, P., Louis, R., Jean-Michel Foidart, Lopez-Otin, C., Noel, A., & Cataldo, D. D. (2010). Matrix Metalloproteinase-19 Deficiency Promotes Tenascin-C Accumulation and Allergen-Induced Airway Inflammation. American Journal of Respiratory Cell and Molecular Biology, 43(3), 286–295. https://doi.org/10.1165/rcmb.2008-0426oc

[33] Hussan Kodakkat Parambil, S., Asharaf Thozhuvana Parambil, H., Parammal Hamza, S., Thirumangalath Parameswaran, A., Shahin Thayyil, M., & Karuvanthodi, M. (202). DFT and molecular docking studies of a set of non-steroidal anti-inflammatory drugs: Propionic acid derivatives. IntechOpen. https://doi.org/10.5772/intechopen.93828

[34] Qureshi, O. & Dua, A. COX Inhibitors. (2022 Sep 12). In: StatPearls [Internet]. Treasure Island (FL): StatPearls Publishing; 2022 Jan-. Available from: https://www.ncbi.nlm.nih.gov/book

[35] Gubernatorova, E. O., & Tumanov, A. V. (2016). Tumor necrosis factor and lymphotoxin in regulation of intestinal inflammation [Abstract]. Biochemistry (Moscow), 81(11), 1309-1325. doi:10.1134/s0006297916110092

[36] Snodgrass, R. G., & Brüne, B. (2019). Regulation and functions of 15-Lipoxygenases in human macrophages. Frontiers in Pharmacology, 10. https://doi.org/10.3389/fphar.2019.00719

[37] Ducharme, Y., Blouin, M., Brideau, C., Châteauneuf, A., Gareau, Y., Grimm, E. L., Juteau, H., Laliberté, S., MacKay, B., Massé, F., Ouellet, M., Salem, M., Styhler, A., & Friesen, R. W. (2010). The discovery of setileuton, a potent and selective 5- lipoxygenase inhibitor. ACS Med Chem Lett, 1(4),170-4. https://doi.org/10.1021/ml100029k.

[38] Martel-Pelletier, J., Lajeunesse, D., Reboul, P., (2003). Therapeutic role of dual inhibitors of 5-LOX and COX, selective and non-selective non-steroidal anti-inflammatory drugs. Annals of Rheumatic Diseases, 62, 501-509.

[39] Pantsar, T., & Poso, A. (2018). Binding Affinity via Docking: Fact and Fiction. Molecules, 23(8), 1899. https://doi.org/10.3390/molecules23081899

[40] Chen, D., Oezguen, N., Urvil, P., Ferguson, C., Dann, S. M., & Savidge, T. C. (2016). Regulation of protein-ligand binding affinity by hydrogen bond pairing. Science Advances, 2(3). https://doi.org/10.1126/sciadv.1501240